JPE 6-3-4

Reduced Rating T-Connected Autotransformer Based Thirty-Pulse AC-DC Converter for Vector Controlled Induction Motor Drives

Bhim Singh*, G.Bhuvaneswari* and Vipin Garg†*

†*Deptt. of Electrical Engg., Indian.Institute of .Technology,.Delhi, New Delhi, India

ABSTRACT

The design and performance analysis of a reduced rating autotransformer based thirty-pulse AC-DC converter is carried out for feeding a vector controlled induction motor drive (VCIMD). The configuration of the proposed autotransformer consists of only two single phase transformers, with their windings connected in a T-shape, resulting in simplicity in design, manufacturing and in a reduction in magnetics rating. The design procedure of the autotransformer along with the newly designed interphase transformer is presented. The proposed configuration has flexibility in varying the transformer output voltage ratios as required. The design of the autotransformer can be modified for retrofit applications, where presently a 6-pulse diode bridge rectifier is used. The proposed thirty-pulse AC-DC converter is capable of suppressing less than 29^{th} harmonics in the supply current. The power factor is also improved to near unity in the wide operating range of the drive. A comparison of different power quality indices at AC mains and DC bus is demonstrated in a conventional 6-pulse AC-DC converter and the proposed AC-DC converter feeding a VCIMD. A laboratory prototype of the proposed autotransformer based 30-pulse AC-DC converter was developed with test results validating the proposed design and system.

Keywords: autotransformer, multipulse ac-dc converter, power quality improvement, VCIMD

1. Introduction

Variable frequency induction motor drives (VFIMDs) are used in various industrial applications such as air conditioning units, pumps for waste water treatment plants, in the cement industry, paper and textile mills, rolling mills etc. [1]. These induction motor drives are generally used in vector control mode due to advantages such as having DC motor characteristics, fast dynamic response, and precise speed control [2]. Vector controlled induction motor drives (VCIMDs) are generally fed from a three-phase diode bridge rectifier resulting in the injection of harmonics in the AC mains, thereby polluting the power quality at the point of common coupling (PCC) [3]. An international standard IEEE 519- 1992 [4] was issued in 1992 placing restrictions on use of these harmonic producing equipments.

To solve these power quality problems, many power factor correction (PFC) approaches have been proposed to shape AC input current waveforms in phase with supply voltage [5]. An active three-phase PFC circuit consisting of semi-conductor switches results in achieving an almost unity power factor operation. But these techniques can not

Manuscript received Sept. 14, 2005; revised May . 4, 2006
†Corresponding Author: vipin123123@gmail.com
Tel: +91-11-26596225 Fax: +91-11-26581086 I. I. T. Delhi
*Dept. of Electrical Eng., Indian Institute of Technology Delhi

be used at high power levels due to the large switching losses incurred at high switching frequencies generally used, apart from the complex control circuit.

On the other hand, passive PFC circuits making use of multipulse AC-DC converters for harmonic reduction are being used to a great extent due to their ruggedness, robustness, high efficiency and simplicity. For applications, where isolation is not required, autotransformer based configurations are cost effective, due to the reduced rating of the autotransformer. Different configurations of 12-pulse and 18-pulse rectification based converters have been reported in the literature [6-11]. Recently, an 18-pulse converter was reported [12] to reduce harmonics, but the THD of the AC mains current was around 8.6%, which deteriorates further at reduced loads. Therefore, these 12-pulse or 18-pulse AC-DC converters may not be suitable for applications where harmonic reduction is stringent. To improve the power quality indices, DC ripple re-injection has also been used with existing 12-pulse AC-DC converters [13-14]. Even with this arrangement, the THD of the supply current is poor under light load conditions. To improve the THD of the AC mains current further, a 28-step current shaper was proposed [15], but even with this configuration, the THD of the AC mains current at full load is 6.54%, which deteriorates under light load conditions.

This paper presents a reduced rating T-connected autotransformer based 30-pulse AC-DC converter feeding vector controlled induction motor drive. The proposed autotransformer makes use of only two main windings, from which different phase voltages at different phase angles are produced. Moreover, the design of the autotransformer is modified to make it suitable for retrofit applications. Additionally, a comparison of different power quality parameters such as total harmonic distortion (THD) and crest factor of AC mains current (CF), power factor (PF), displacement factor (DPF) and distortion factor (DF), THD of supply voltage at PCC, ripple factor (RF) at DC bus is made for the VCIMD fed conventional 6-pulse AC-DC converter (Topology 'A') and the proposed thirty-pulse AC-DC converter. The autotransformer suitable for the T connected 30-pulse AC-DC converter was developed in the laboratory and various tests were conducted on the developed prototype to validate the simulated results.

2. Design and Analysis of Proposed T-Connected Autotransformer Based Thirty-Pulse AC-DC Converter

Harmonic elimination through a non-isolated transformer makes use of two or more converters, where the harmonics generated by one converter are cancelled by the other converter through a proper phase shift given by:

Phase shift = 60^0/ Number of six-pulse converters

To achieve 30-pulse rectification, the phase shift required between any two nearby sets of voltages is of 12^0. The complete circuit consisting of the proposed autotransformer, diode bridge rectifiers, interphase transformers and the VCIMD is shown in Fig.1. Three-phase AC voltages are given to the autotransformer, which produces 5-sets of three-phase voltages of same magnitude and distributed in time through phase shifts of 12^0, as shown in Figs.2a and 2b. The parts design of the proposed converter is discussed following.

2.1 Design of T-connected autotransformer

The T-connected autotransformer makes use of only two main windings (compared to the three main winding transformers reported earlier) resulting in reduced space, size, volume, weight and cost. The two main windings AD and CB are connected as shown in Fig. 1. The ratio of number of turns in windings AD (N_1) and CB (N_2) is given as [16]:

$$N_1/ N_2 = 0.866 \quad (1)$$

The phase shifted voltages produced by the autotransformer are shown in the phasor diagram in Fig.2a. The desired phase shift for the 30-pulse converter operation is achieved by connecting different segments of windings AD and CB at suitable taps. The required number of turns in the different segments of windings AD and CB are calculated as follows: Define winding constants $K_1, K_2, K_3, K_4, K_5, K_6$ being the fractions of phase voltage V_{AN} and the winding constants $K_7, K_8, K_9, K_{10}, K_{11}, K_{12}$ being the fractions of line voltage $V_{BC}/2$.

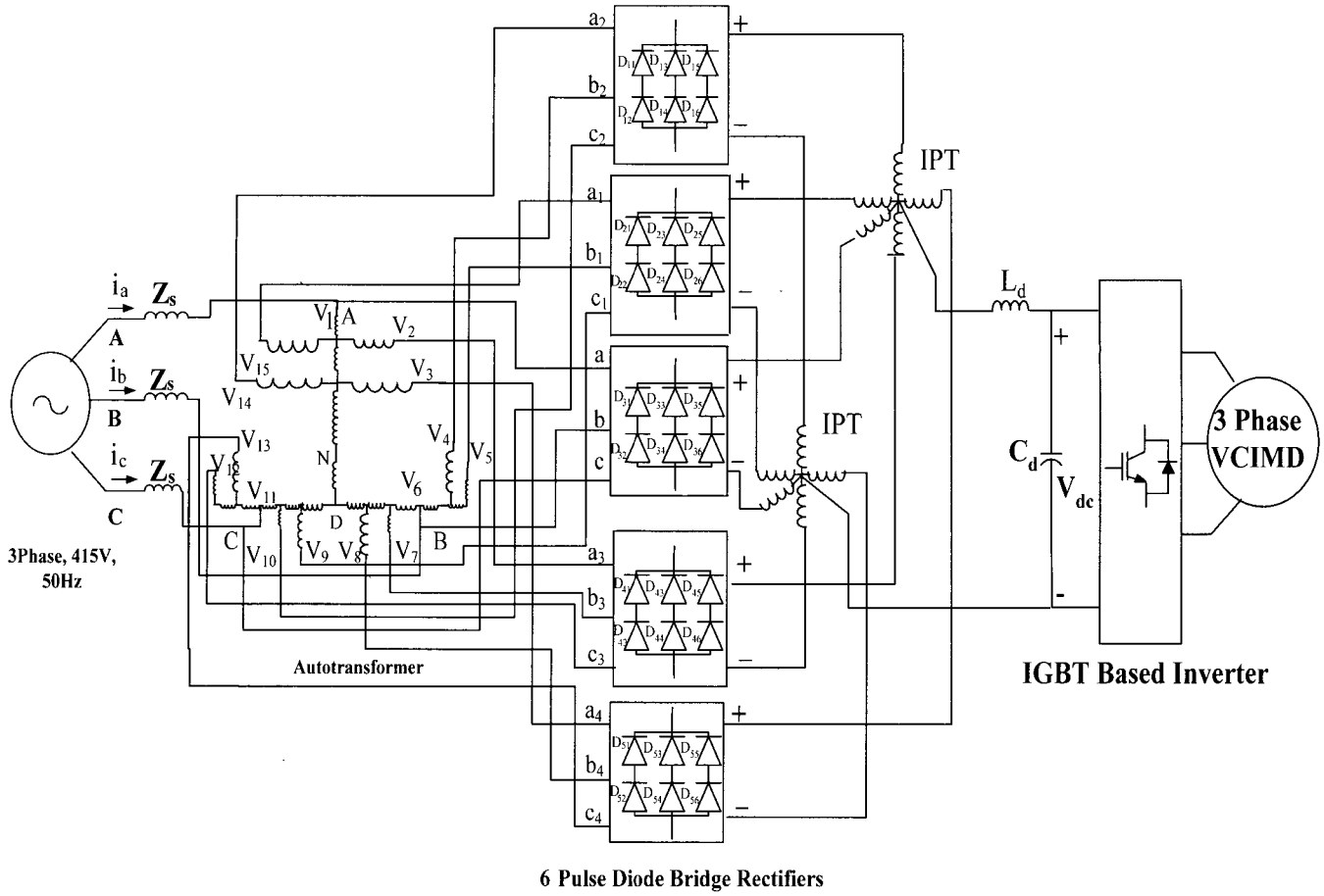

Fig. 1 The proposed 30-pulse ac-dc converter based on T-connected autotransformer feeding VCIMD (Topology 'B').

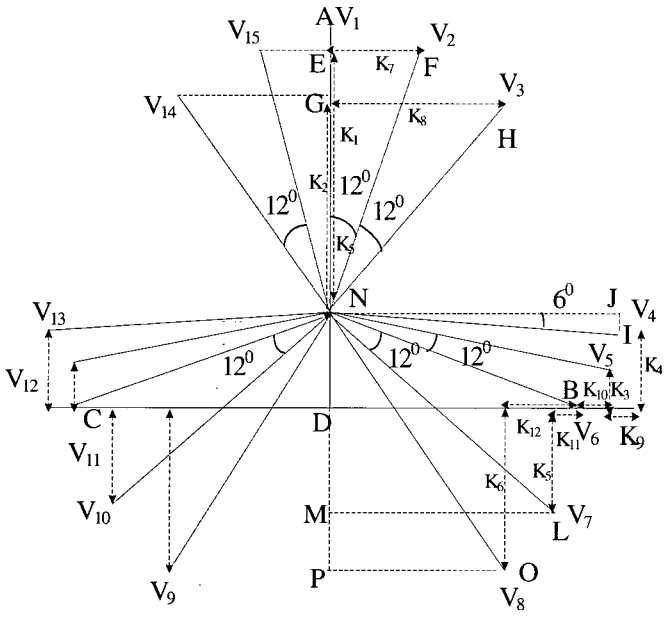

Fig. 2a Phasor diagram of voltages in the proposed autotransformer connection.

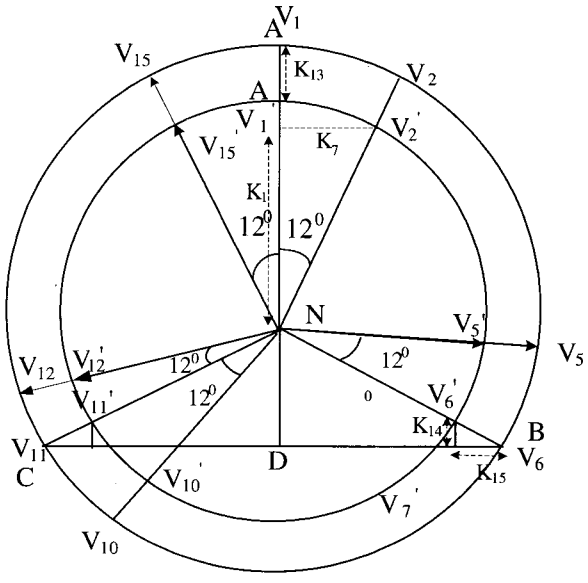

Fig. 2b Generalized vector diagram for retrofit arrangement.

Consider Phase 'A', the voltage V_2 is to be produced at an angle of -12^0 with respect to V_1. From the phasor diagram in Fig.2a, one can write it as:

$V_{NE}/V_{NF} = Cos12^0$, $V_{NE} = K_1 V_A = V_{NF} Cos12^0 = V_A Cos12^0$, giving, $K_1 = Cos12^0 = 0.978$ (2)

Similarly, $V_{EF}/V_{NF} = \sin 12^0$, $V_{EF} = K_7 V_{BC} = V_A \text{ Sin } 12^0$, giving

$K_7 = Sin12^0 /1.732 = 0.12$ (3)

Phase voltage V_3 is at an angle of 12^0 lag with respect to V_2. To produce V_3, winding constants K_2 and K_8 are calculated, which is similar to K_1 and K_2. These winding constants emerge as $K_2 = 0.9135$, $K_8 = 0.2348$. The phase voltages V_{15} and V_{14} are mirror images of phase voltages V_2 and V_3. Thus, the same winding constants may be used to connect the winding tappings at the desired positions.

In considering Phase 'B', voltage V_4 is at an angle of 24^0 leading with respect to V_B (= V_6) and V_7 is at an angle of -12^0 with respect to V_B. To produce V_4 and V_7, winding constants K_5, K_{11}, K_4 and K_9 are calculated.

From triangle NML,

$ML /NL = Sin 48^0$, $ML = V_{BC}/2 - K_{11} V_{BC}/2 = V_B \text{ Sin } 48^0$, giving $K_{11} = 0.3581$ (4)

Also, $MN/NL = Cos 48^0$, $MN = V_B Cos 48^0$,

$K_5 V_A = DM = MN\text{-}ND = (V_B Cos 48^0 - V_A/2)$ giving

$K_5 = 0.1691$ (5)

From triangle NIJ, $NJ/NI = Cos 6^0$,

$NJ = V_B Cos6^0$; $K_9 V_{BC}/2 = (V_B Cos6^0 - V_{BC}/2)$, giving

$K_9 = 0.1483$ (6)

$IJ/NI = Sin 6^0$, $IJ = V_B Sin 6^0$ giving

$K_4 = (ND - V_B Sin6^0)/ V_A$, thus resulting in

$K_4 = 0.3954$ (7)

Similarly, phase voltage V_5 is at -12^0 with respect to V_4. To produce V_5, winding constants K_3 and K_{10} are calculated. The winding constant K_{10} emerge as 0.0999 and K_3 is 0.1909. Again phase voltages V_9, V_{10}, V_{12} and V_{13} are mirror images of phase voltages V_8, V_7, V_5 and V_4 respectively. Therefore, these voltages may also be produced from these winding constants.

With this arrangement, the autotransformer produces five sets of three-phase voltages of equal magnitude but shifted in phase through 12^0. However, the DC link voltage obtained is higher than that of a 6-pulse diode bridge rectifier output by about 5.0% due to the 30-pulse rectification. To make the proposed autotransformer suitable for retrofit applications it is modified. The design modifications are explained below.

Fig.2b shows a generalized diagram of various phase voltages for achieving different voltage ratios from the autotransformer by varying the tap positions in the proposed autotransformer. This ensures that the output voltages still have the required phase shift of 12^0 (for achieving the desired 30-pulse operation). For the retrofit arrangement, the supply voltages are on the outer circle, whereas the phase shifted output voltages are on the inner circle in Fig.2b. The inner circle is located at 0.95 of the outer circle. Thus, the new tap positions can be calculated from the same winding constants given above. But, the only change is that the input voltages are reduced by 5%. Accordingly, all the winding voltages can be found except voltages V_1, V_6 and V_{11}. To calculate these voltages, new winding constants K_{13}, K_{14} and K_{15}, as shown in Fig.2b are calculated. These constants emerge as K_{13} = 0.05, K_{14} = 0.025 and K_{15} = 0.05. Thus, by simply changing the transformer winding tapping, as shown in Fig.2b, the same DC link voltage as that of the 6-pulse diode bridge rectifier is obtained. The proposed multiphase AC-DC converter along with the redesigned autotransformer for retrofit applications is shown in Fig.3 and referred to as Topology 'C'. The current flowing through the different segments of the windings along with their respective phase currents are shown in Fig.4. It shows improvement in the supply current due to the phase shift achieved in different winding currents.

The kVA rating of the transformer is calculated as [6]:

$$kVA = 0.5\sum V_{winding} \quad I_{winding} \tag{8}$$

The kVA rating of the interphase transformer is also calculated using the above relationship.

2.2 Design of interphase transformer

The five sets of voltages produced by the autotransformer are transferred to the three-phase diode rectifier bridges, which rectify these voltages. The obtained DC voltages are also phase shifted through an angle of 12^0. These voltages are applied to the interphase transformer (IPT) to ensure the independent operation of the rectifier circuits, as shown in Fig.5a. Figure 5b shows

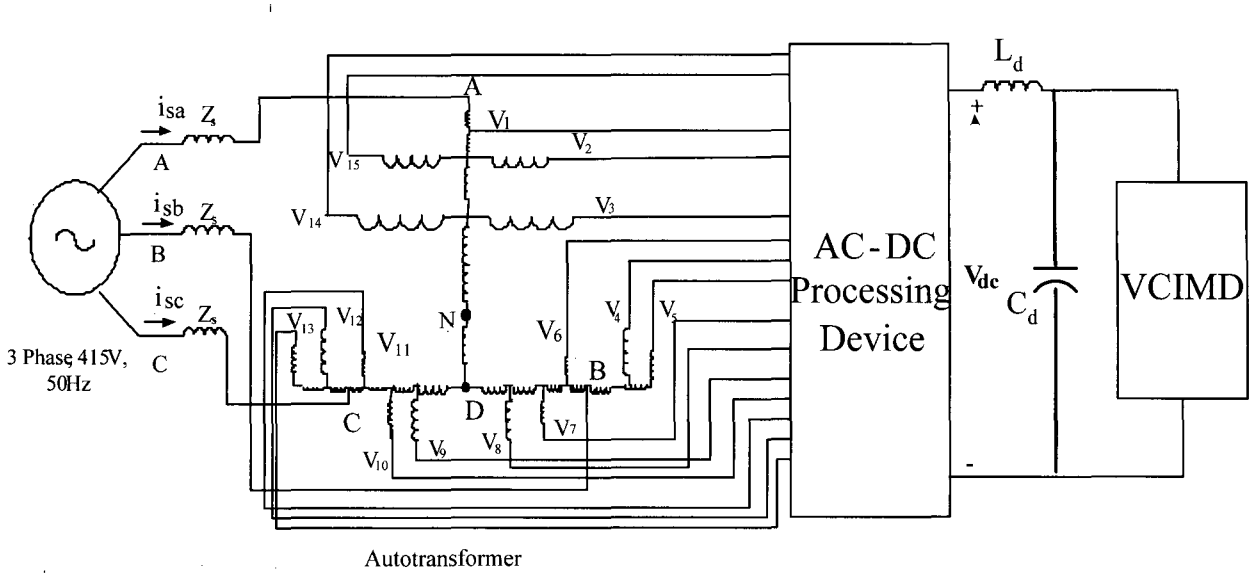

Fig. 3 Proposed 30-pulse ac-dc converter fed VCIMD for retrofit applications (Topology 'C').

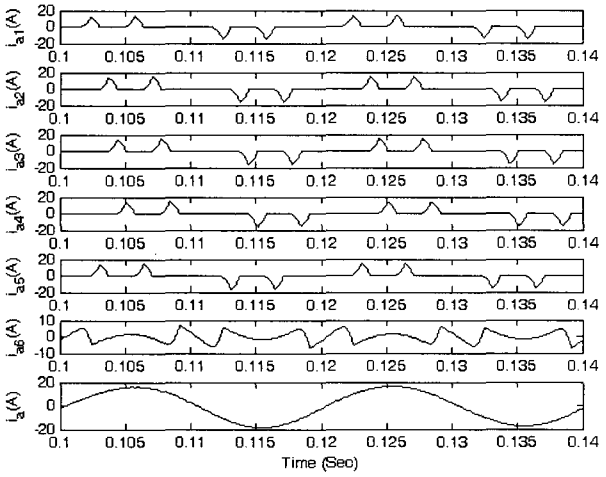

(a)

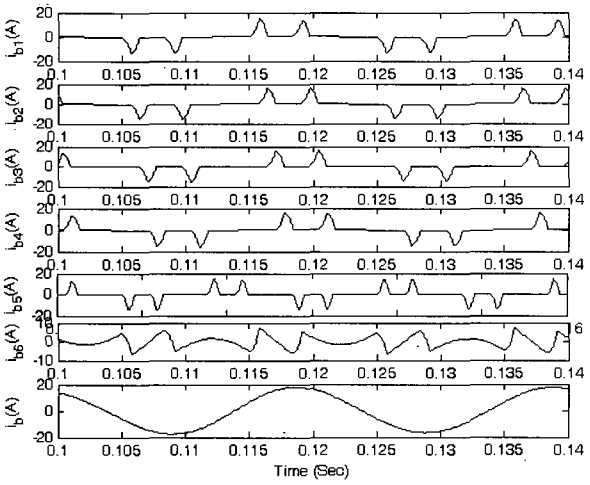

(b)

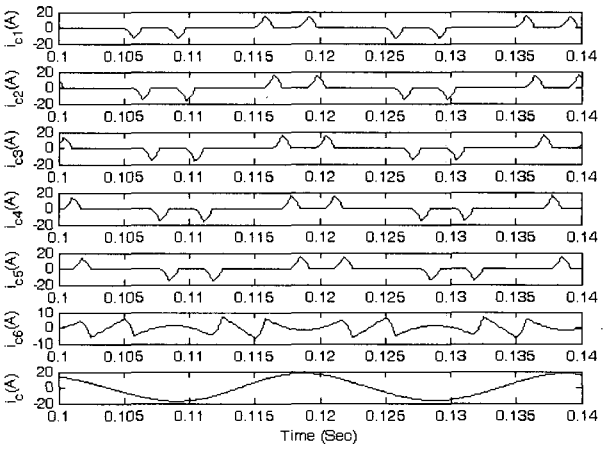

(c)

Fig. 4 Waveforms of different winding currents alongwith supply current for phase (a) A, (b)B, (c) C at full load for Topology 'C'.

the detailed winding configuration of the interphase transformer. It consists of a five legged core with five closely coupled windings. The close coupling of the windings ensures an mmf balance as in a transformer, forcing the load current to divide equally among all the windings. Thus, each winding of the interphase transformer carries one fifth of the load current, thus leading to a rating reduction of the interphase transformer. The IPT ensures symmetric conduction of each diode of all the rectifier bridges, as shown in Fig.6.

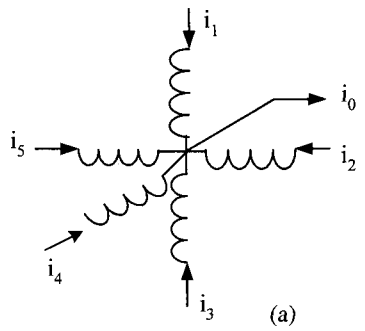

Fig. 5 Winding configuration of interphase reactor

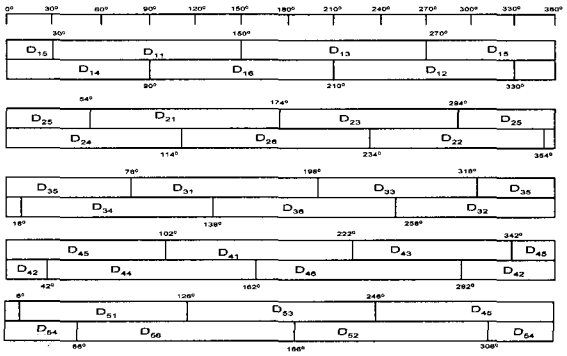

Fig. 6 Diode conduction sequence diagram

3. Modeling of Vector Controlled Induction Motor drive

Fig.7 shows the schematic diagram of a 6-pulse AC-DC converter fed indirect vector controlled induction motor drive, referred as Topology 'A'. The motor is controlled in vector control mode using an indirect vector control technique, due to its advantages. To realize the vector control of an induction motor, two motor phase currents namely i_{as} and i_{bs} and the motor speed signal (ω_r) are sensed. The closed loop PI speed controller compares the reference speed (ω_r^*) with motor speed (ω_r) and generates reference torque $T_{(n)}^*$(after limiting it to a suitable value).

$$T^*_{(n)} = T^*_{(n-1)} + K_p \{\omega_{e(n)} - \omega_{e(n-1)}\} + K_I \omega_{e(n)} \quad (9)$$

where, $T^*_{(n)}$ and $T^*_{(n-1)}$ are the output of the PI controller (after limiting it to a suitable value) and $\omega_{e(n)}$ and $\omega_{e(n-1)}$ are the speed error signals at the n^{th} and $(n-1)^{th}$ instants. K_p and K_I are the proportional and integral gain constants.

The exciting current is governed by the speed of the induction motor and is expressed as:

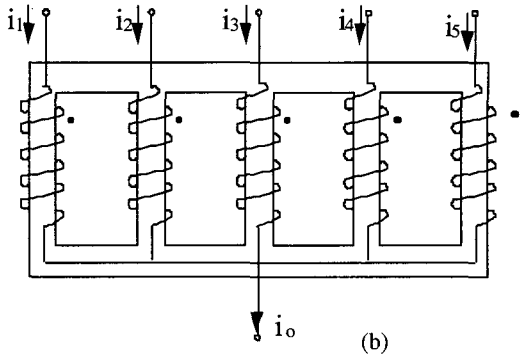

$$i_{mr} = I_{mr} \quad \text{if} \quad \omega_r < \omega_s \quad (10)$$

$$i_{mr} = I_{mr} (\omega_r / \omega_s) \quad \text{if} \quad \omega_r > \omega_s \quad (11)$$

where I_{mr} is the rated exciting current and ω_s is the base synchronous speed of an induction motor.

The flux control signal (i_{mr}) along with $T^*_{(n)}$ are fed to the vector controller, which computes the flux producing component of current (i_{ds}^*), torque component of current (i_{qs}^*), slip speed (ω_2^*) and the flux angle (ψ) as given below:

$$i_{ds}^* = i_{mr} + \tau_r (\Delta i_{mr}/\Delta T) \quad (12)$$

$$i_{qs}^* = T^*/(k\, i_{mr}) \quad (13)$$

$$\omega_2^* = i_{qs}^*/(\tau_r\, i_{mr}) \quad (14)$$

$$\Psi_{(n)} = \Psi_{(n-1)} + (\omega_2^* + \omega_r)\, \Delta T \quad (15)$$

where K is a constant, it depends on motor parameters, $\Psi_{(n)}$ and $\Psi_{(n-1)}$, the value of rotor flux angles at n^{th} and $(n-1)^{th}$ instants respectively and ΔT is the sampling time, which is taken as 100 μ secs.

These currents (i_{ds}^*, i_{qs}^*) in a synchronous rotating frame are converted to a stationary frame three phase currents (i_{as}^*, i_{bs}^*, i_{cs}^*) as given below:

$$i_{as}^* = -i_{qs}^* \sin\Psi + i_{ds}^* \cos\Psi \quad (16)$$

$$i_{bs}^* = \{-\cos\Psi + \sqrt{3}\sin\Psi\} i_{ds}^* (1/2) + \{\sin\Psi + \sqrt{3}\cos\Psi\} i_{qs}^* (1/2) \quad (17)$$

$$i_{cs}^* = -(i_{as}^* + i_{bs}^*) \quad (18)$$

These reference currents (i_{as}^*, $i_{bs}^*$and i_{cs}^*), generated by the vector controller, are compared with sensed motor currents (i_{as}, i_{bs} and i_{cs}). The calculated current errors are amplified and fed to the PWM current controller, which controls the gating of the different switches in VSI. The VSI generates the PWM voltages being fed to the motor to develop the torque required to maintain a rotor speed equal to the reference speed.

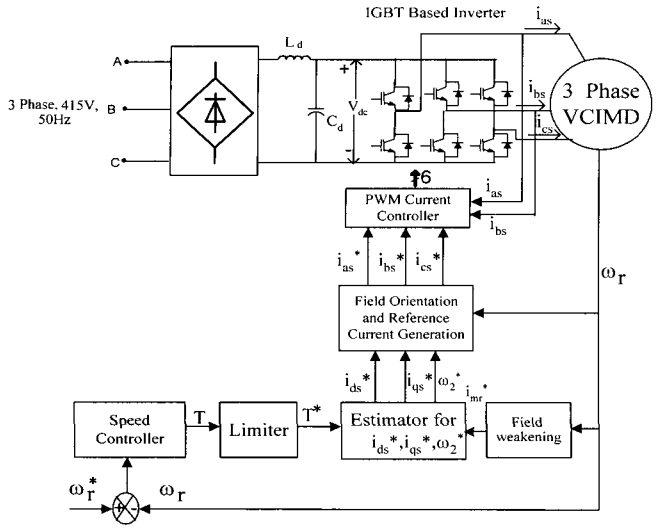

Fig. 7 Six-pulse diode bridge rectifier fed vector controlled induction motor drive. (Topology A).

4. MATLAB Based Simulation

The complete system comprising of the proposed autotransformer based ac-dc converter feeding VCIMD is simulated in MATLAB environment along with Simulink and Power System Blockset (PSB) toolboxes. The MATLAB model of the proposed ac-dc converter feeding VCIMD is shown in Fig.8. Fig.9 shows the MATLAB model of the sub-block of the vector controlled induction motor drive. The VCIMD consists of a 10 hp, 415V induction motor drive (detailed data are given in Appendix) controlled using indirect vector control technique. The source impedance has been kept at a practical value of 3% in all the simulations.

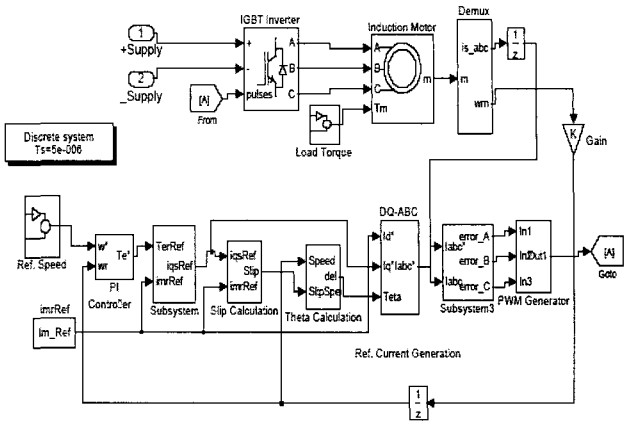

Fig. 9 MATLAB block diagram of VCIMD

5. Experimentation

The simulated results were verified on a test bench consisting of the newly designed and developed autotransformers along with small rating interphase transformers as shown in Fig.5. Two single phase autotransformers were designed and wound in the laboratory as per the design details given below:

Flux density = 0.8 Tesla, Current density = 2.3A/m^2, Core Size = 8 No., Area of cross section of core = 5161mm^2. Size of E-Laminations is (120mm X 188mm) and that of I-laminations is (188mm X 25mm). Number of turns per volt = 1. Accordingly, different windings (shown in Fig.3) of different cross sections for the proposed 30-pulse converter were wound for both the single phase transformers.

Similarly, the interphase transformers of the small ratings were designed and developed. Various tests were carried out at three-phase line voltage of 230V AC input

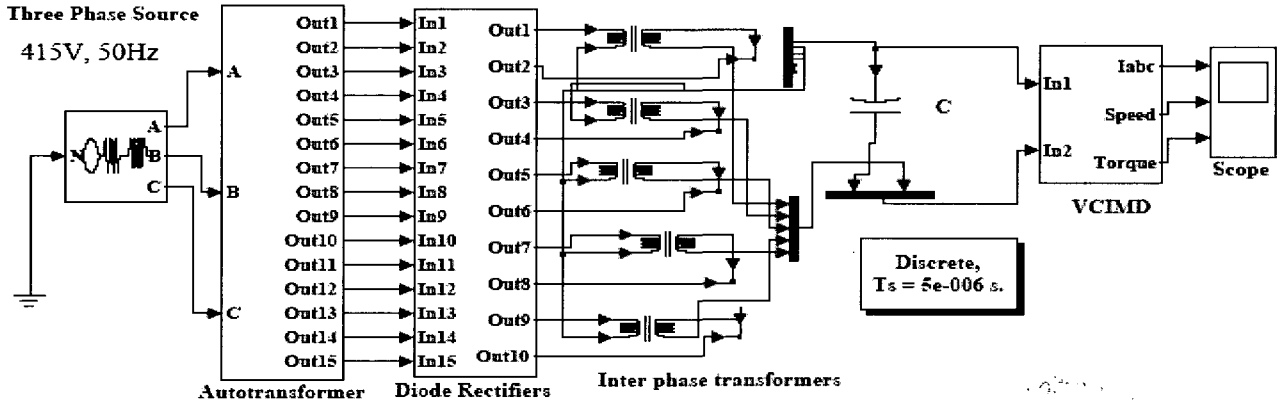

Fig. 8 MATLAB block diagram of proposed 30-pulse ac-dc converter fed VCIMD (Topology 'C')

and with an equivalent resistive load. The test results were recorded using Fluke make power analyzer model 43B on the developed prototype of the T-connected autotransformer based thirty-pulse AC-DC converter.

6. Results and Discussion

To compare the performance of the proposed thirty-pulse AC-DC converter with the existing 6-pulse AC-DC converter, first a 6-pulse diode bridge rectifier fed VCIMD was designed, modeled and simulated. The dynamic performance of the drive along with load perturbation on the VCIMD is shown in Fig.10. The set of curves consists of supply voltage v_s, supply current i_s, three-phase motor current i_{abcs}, motor developed torque 'T_e' (in N-m), rotor speed 'ω_r' (in electrical rad /sec) and DC link voltage v_{dc} (V). The supply current waveform along with its harmonic spectrum at full load is shown in Fig.11, showing the THD

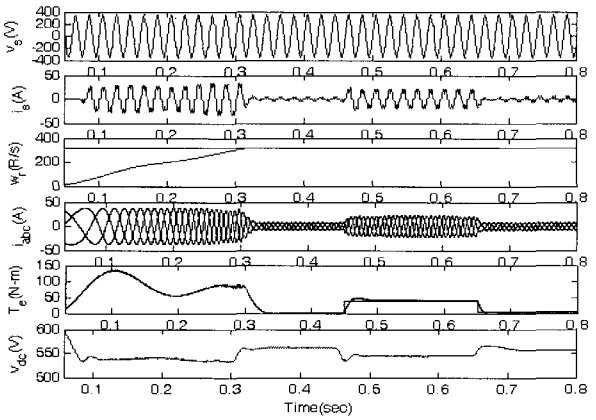

Fig. 10 Dynamic response of 6-pulse diode rectifier fed VCIMD with load perturbation. (Topology 'A').

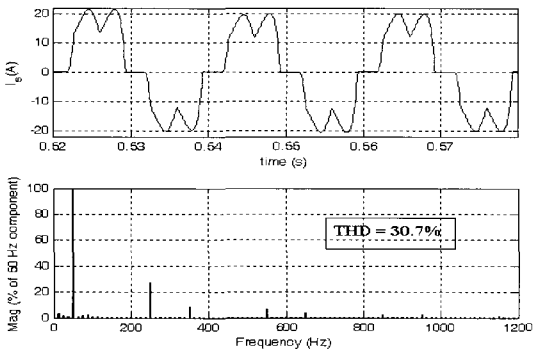

Fig. 11 AC mains current waveform along with its harmonic spectrum at full load in Topology 'A'

of the AC mains current as 30.7%. The THD of the AC mains current deteriorates to 57.2% at light load (20%) as shown in Fig.12. Furthermore, the power factor at full load is 0.935, which deteriorates to 0.807 at light load, (as shown in Table-I). These power quality indices are not within IEEE Standard 519 limits [4]. These results indicate the need for an improved power quality AC-DC converter.

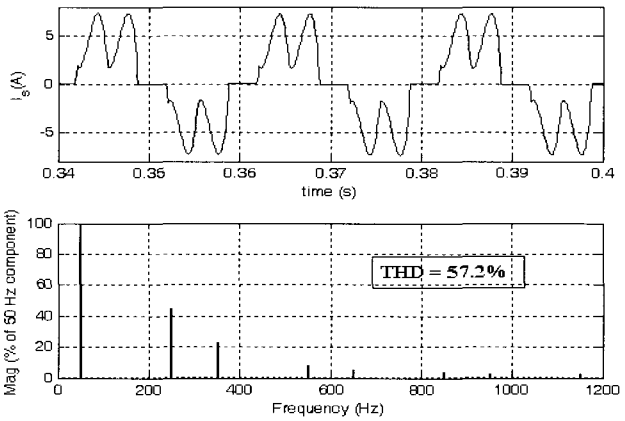

Fig. 12 AC mains current waveform along with its harmonic spectrum at light load in Topology 'A'.

6.1 Performance of Proposed Thirty-Pulse AC-DC Converter Fed VCIMD

To improve the performance of the existing drive, a T-connected autotransformer based thirty-pulse AC-DC converter was modeled, designed and simulated in a MATLAB environment and is referred to as Topology 'B'. In this Topology, the DC link voltage is higher than that of a 6-pulse diode bridge rectifier, due to thirty-pulse rectification, as given in Table-I. The design of the autotransformer was modified for retrofit applications, as explained earlier, resulting in Topology 'C'. This Topology is similar to Topology 'B' except for the difference in number of turns in the different windings.

The improved performance of the drive is shown graphically in Figs.13-17 and quantitatively in Tables I-II. The dynamic performance of the proposed AC-DC converter fed VCIMD (Topology 'C') is shown in Fig.13, showing similarities in dynamic response as well as improvement in supply current waveform. The waveform of the supply current at full load along with its harmonic spectrum demonstrates additional improvements and is

shown in Fig.14. It clearly shows the elimination of harmonics in supply current resulting in improvement in THD. Under light load conditions (20% of full load), the waveform of the supply current along with its harmonic spectrum is shown in Fig.15. It was observed that all the harmonic components are always less than 8% of fundamental current, thus easily meeting IEEE standards [4].

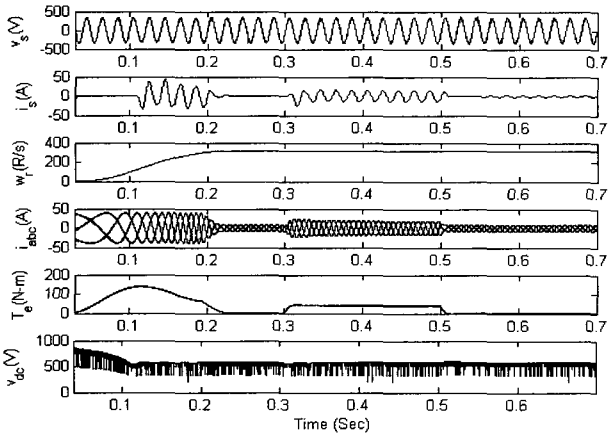

Fig. 13 Dynamic response of proposed ac-dc converter (Topology 'C') fed VCIMD with load perturbation.

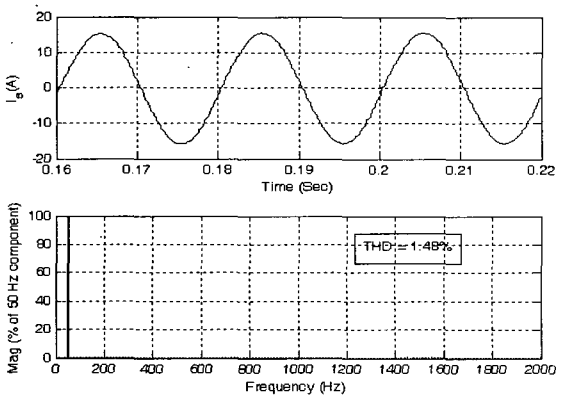

Fig. 14 AC mains current waveform alongwith its harmonic spectrum at full load for Topology 'C'

To demonstrate the capability of the proposed 30-pulse AC-DC converter under load variations on the VCIMD, the load is varied on the VCIMD and its effect on various power quality indices is also shown in Table-II. It can also be observed from Table-II that the proposed converter results in a near unity power factor in wide operating ranges of the drive and the THD of supply current is always less than 5%. This is within the IEEE Standard 519 limits [4].

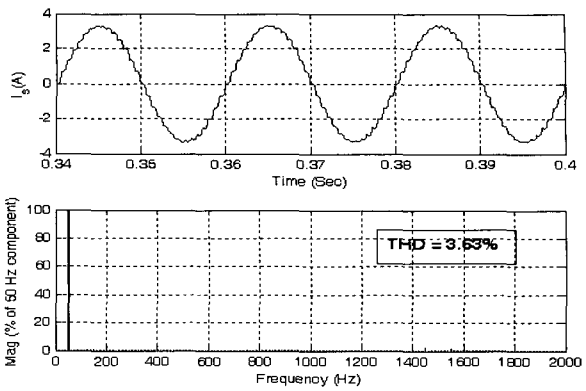

Fig. 15 AC mains current waveform alongwith its harmonic spectrum at light load for Topology 'C'

The comparison of the different power quality indices of the VCIMD fed 6-pulse AC-DC converter and the proposed AC-DC converter is shown in Table I. This table shows the quantitative improvement in these indices for the proposed AC-DC converter. It is also observed from Table-I, that the rms current drawn from the three-phase AC mains decreased reasonably as compared to that in the 6-pulse AC-DC converter fed system under the same full load and light load conditions. Moreover, there is improvement in the DC link voltage regulation. There was appreciable improvement in the ripple factor (RF) on the DC bus. Additionally, it leads to size reduction in the DC capacitor for maintaining the same ripple factor. The variation of % THD of the AC mains current and power factor (PF) with load on the 6–pulse VCIMD and the proposed 30-pulse AC-DC converter is shown in Figs.16 and 17 respectively, graphically showing the improvement in these power quality indices.

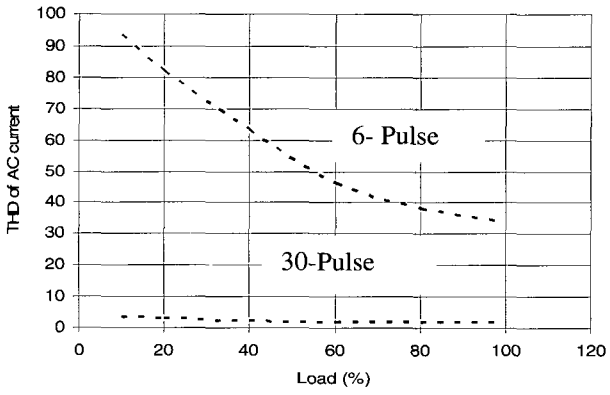

Fig. 16 Variation of THD of ac mains current with load in Topologies 'A' and 'C'

Table 1 Comparison of power quality parameters of a VCIMD fed from different converters

Sr. No.	Topology	THD V_s (%) Full Load	I_s (A)		Total Harmonic Distortion (THD) of I_s (%)		Distortion Factor (DF)		Displacement Factor (DPF)		Power Factor (PF)		DC Link Voltage(V) Average	
			Full Load	Light Load (20%)	Full Load	Light Load (20%)	Full Load	Light Load (20%)	Full Load	Light Load (20%)	Full Load	Light Load (20%)	Full Load	Light Load (20%)
1.	6-Pulse (A)	8.29	13.8	4.09	30.7	57.2	.955	.868	.980	.959	.935	.807	547	555
2.	30-Pulse (B)	2.13	10.9	2.46	1.53	3.60	.999	.999	.994	.995	.993	.994	576	582
3.	Proposed (C)	1.80	10.9	2.34	1.48	3.63	.999	.999	.998	.994	.994	.997	547	553

Table 2 Comparison of power quality indices of proposed 30-pulse harmonic mitigator (Topology 'C') fed VCIMD under varying loads.

Load (%)	THD (%)		CF of I_s	DF	DPF	PF	RF (%)	V_{dc} (V)
	I_s	V_t						
20	3.63	0.96	1.43	.999	.998	.997	.003	553
40	3.06	1.30	1.42	.999	.996	.995	.005	552
60	2.62	1.51	1.42	.999	.992	.991	.006	550
80	1.97	1.63	1.42	.999	.991	.990	.007	548
100	1.48	1.80	1.42	.999	.995	.994	.009	547

Table 3 Experimental comparison of power quality indices of proposed 30-pulse harmonic mitigator (Topology 'C') under varying loads.

I_s(A)	THD (%)		CF of I_s	DF	DPF	PF	V_{dc} (V)
	I_s	V_t					
3.58	4.3	1.0	1.4	.999	.99	.99	298
4.86	3.9	1.1	1.4	.999	.99	.99	294
7.92	3.2	1.2	1.4	.999	.99	.99	288
9.19	3.0	1.3	1.4	.999	.99	.99	285
11.6	2.9	1.4	1.4	.999	.99	.99	282

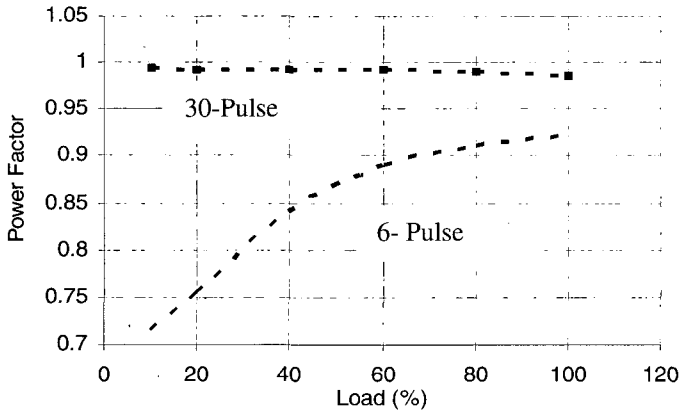

Fig. 17 Variation of power factor with load in Topologies 'A' and 'C'.

On the magnetics front, there is also a reduction in rating, as it needs an autotransformer of 3.0kVA and an interphase transformer of 0.62kVA, totaling the magnetics rating to only 34.6% of the drive rating. It further results in savings in volume, size and finally the cost of the drive.

6.2 Experimental Performance of Proposed 30-Pulse AC-DC Converter (Topology 'C')

Various tests were carried out on the developed prototype for Topology 'C', shown in Fig.18. The experiments were carried out with an equivalent resistive load at a reduced voltage of 230V and with the same current level. The waveform of supply voltage (v_{ab}) and supply current (i_c) along with the harmonic spectrum of the AC mains current at full load in Topology 'C' is shown in Fig. 18a and at light load (25%) it is shown in Fig.18b. The THD of the AC mains current at full load was observed at 2.9% and under light load was 4.3%. The effect of load variation on different power quality indices in Topology 'C' is shown in Table-III. The test results show similar trends as in the simulated results, thus validating the developed design procedure and simulation model of the proposed 30-pulse AC-DC converter.

7. Conclusions

The design, modeling, simulation and experimental validation of a novel T-connected autotransformer based 30-pulse AC-DC converter was presented for feeding a VCIMD. The proposed autotransformer based AC-DC converter resulted in eliminations less than the 29^{th} harmonic in the supply current. The design technique of the proposed converter shows the flexibility of the autotransformer design for retrofit applications.

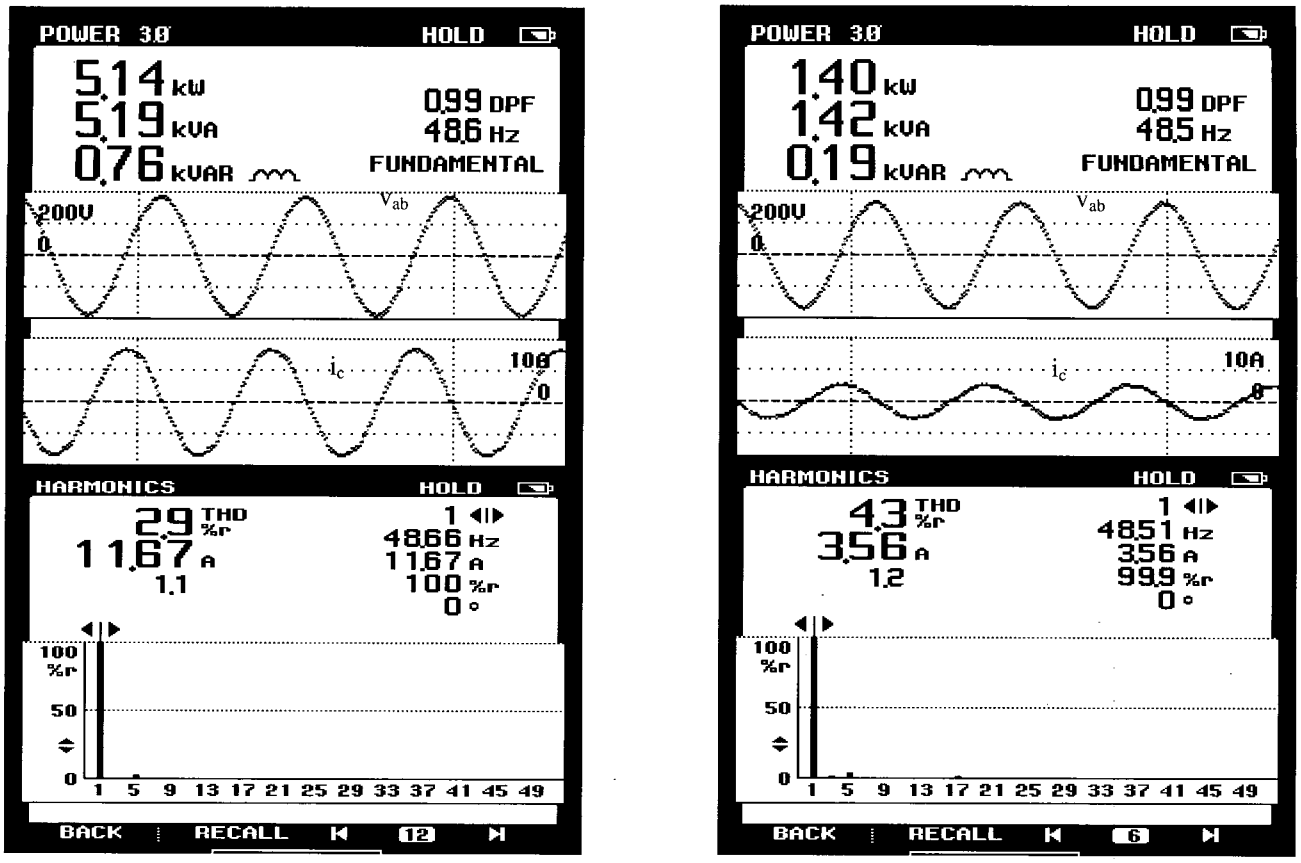

(a) (b)

Fig. 18 Recorded waveforms of 30-pulse ac-dc converter system
(a) supply voltage (v_{ab}) and current waveforms (i_c) and harmonic spectrum of supply current at full load,
(b) supply voltage (v_{ab}) and current waveforms (i_c) and harmonic spectrum of supply current at light load.

There have been drastic improvements in the THD, crest factor and rms value of the AC mains current, as well as in the power factor in the wide operating range of the drive. The proposed thirty-pulse AC-DC converter has resulted in reduction in magnetics rating leading to saving in cost, weight, volume and size.

Appendix

Motor data:

Three- Phase Squirrel Cage Induction Motor –10 hp (7.5kW), 3-Phase, 4 Pole, Y- connected, 415 V, 50 Hz, rated current = 14.5A, R_s = 1.0 ohms, R_r = 0.76 ohms, X_{ls} = 0.77 ohms, X_{lr} = 0.77 ohms, X_m = 18.84 ohms, J= 0.1 kg-m^2

PI Speed Controller: K_p = 7.0, K_I = 0.1

DC link parameters: L_d = 0.002H, C_d = 2200μF.

References

[1] B.K.Bose, "Recent advances in power electronics", IEEE Trans. on Power Electronics, Vol.7, No.1, pp. 2~16, Jan.1992.

[2] P.Vas, Sensorless vector and direct torque control, Oxford University Oxford University Press, 1998.

[3] D.A.Jarc and R.G.Schieman, "Power line considerations for variable frequency drives", IEEE Trans. Ind. Electron., Vol. 45, No. 4, pp.1099~1105, Sept.1985.

[4] IEEE Guide for harmonic control and reactive compensation of Static Power Converters IEEE Standard 519-1992.

[5] Bhim Singh, B.N.Singh, Ambrish Chandra, Kamal

Al-Haddad, Ashish Pandey and Dwarka P.Kothari, "A review of three-phase improved power quality ac-dc converters", IEEE Trans. Ind. Electronics., Vol. 51, No. 3, pp. 641~660, June 2004.

[6] D. A. Paice, Power Electronic Converter Harmonics: Multipulse Methods for Clean Power, New York, IEEE Press, 1996.

[7] D.A. Paice, "Multipulse converter system", U.S. Patent No. 4876634, Oct. 24, 1989.

[8] D.A.Paice, "Transformers for multipulse AC/DC converters", U.S. Patent No. 6101113, 8 August 2000.

[9] J.Ferens, H.D.Hajdinjak and S.Rhodes, "18-pulse rectification system using a wye connected autotransformer," U.S. Patent No. 6,650,557 B2, Nov.18, 2003.

[10] G. R. Kamath, D. Benson and R. Wood, "A novel autotransformer based 18-pulse rectifier circuit," in Proc., IEEE IECON'02, 2002, pp. 795~801.

[11] K.Oguchi and T.Yamada, "Novel 18-pulse diode rectifier circuit with non-isolated phase shifting transformers," IEE Proc. Electr. Power Appl. Vol.14, No.1, Jan.1997. pp.1~5.

[12] F.J.M.de Seixas and I.Barbi, "A 12 kW three-phase low THD rectifier with high frequency isolation and regulated dc output," IEEE Trans. on Power Electronics, Vol.19, No.2, March 2004, pp.371~377.

[13] Shota Miyairi, Shoji Iida, Kiyoshi Nakata and Shideo Masukawa, "New method for reducing harmonics involved in input and output of rectifier with interhase transformer," IEEE Trans. on Industry Applications, Vol.22, No.5, Oct. /Nov.1986, pp. 790~97.

[14] M.E.Villablanca and J.A. Arrilaga, "Pulse multiplication in parallel converters by multi tap control of interphase reactor," IEE Proceeding-B, Vol.139, No.1, Jan.1992, pp 13~20.

[15] C.L.Chen and G.K.Horng, "A new passive 28-step current shaper for three-phase rectification," IEEE Trans. on Industrial Electronics, Vol.47, No.6, December 2000, pp.1212~1219.

[16] M.G.Say, The Performance and Design of Alternating Current Machines, New York, Pitman Publishers, 1962.

Bhim Singh was born in Rahamapur, U. P., India in 1956. He received B. E. (Electrical) degree from University of Roorkee, India in 1977 and M. Tech. and Ph. D. degrees from IIT, Delhi, in 1979 and 1983, respectively. In 1983, he joined as a Lecturer and in 1988 became a Reader in the Department of Electrical Engineering, University of Roorkee. In December 1990, he joined as an Assistant Professor. became an Associate Professor in 1994 and Professor in 1997 at the Department of Electrical Engineering, IIT Delhi. His field of interest includes power electronics and control of electrical machines. Prof. Singh is a Fellow of Indian National Academy of Engineering, Institution of Engineers (India) and Institution of Electronics and Telecommunication Engineers, a Life Member of Indian Society for Technical Education, System Society of India and National Institution of Quality and Reliability and Senior Member IEEE (Institute of Electrical and Electronics Engineers).

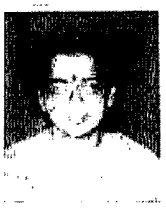

G. Bhuvaneswari received M. Tech. and Ph. D. degrees from IIT, Madras in 1988 and 1992, respectively. In 1997, she joined as an Assistant Professor at the Department of Electrical Engineering, IIT Delhi. Her field of interest includes power electronics, electrical machines and drives, active filters, and power conditioning. She is a fellow of Institution of Electronics and Telecommunication Engineers and Senior Member IEEE (Institute of Electrical and Electronics Engineers).

Vipin Garg received B. Tech. (Electrical) and M.Tech. degrees from NIT, Kurukshetra, India in 1994 and 1996 respectively. In 1995, he joined as a Lecturer in the Department of Electrical Engineering, NIT, Kurukshetra. In January 1998, he joined IRSEE (Indian Railways Service of Electrical Engineers) as an Assistant Electrical Engineer and became Deputy Chief Electrical Engineer in 2006. His field of interest includes power electronics power conditioning and electric traction. He is member of IEEE (Institute of Electrical and Electronics Engineers).